Imaging with Marchenko focusing functions in acoustic and elastic media

Carlos Alberto da Costa Filho (University of Edinburgh)*, Giovanni Angelo Meles (Delft University of Technology, formerly University of Edinburgh) and Andrew Curtis (University of Edinburgh)

Abstract

Applications of the Marchenko method have recently been developed for migration, wavefield redatuming, internal multiple subtraction, and primaries estimation. Marchenko methods estimate the subsurface-to-surface point-source Green's functions and the so-called focusing functions. Focusing functions are solutions of the wave equation which focus in time and space at specified subsurface locations. Here, we use these focusing functions as virtual source/receiver surface acquisition wavefields, with the upgoing focusing function being the virtual received wavefield, created when the downgoing focusing function acts as the source. This results in three imaging schemes, one of which allows individual reflectors chosen to be imaged. These methods provide images with certain advantages over current reverse-time migration methods, such as fewer artifacts, and artifacts that occur in different locations. We show that one of these images can be combined with standard images to remove acquisition and multiple-related artifacts. We demonstrate our methods with acoustic and elastic synthetic examples.

Introduction

Seismic migration is an integral part of seismic exploration, whereby images of the subsurface can be obtained from recorded seismic data. In a standard seismic acquisition, outwards-expanding waves are created by surface sources, which are recorded at a receiver array. An image may be constructed using reverse-time migration (RTM), where a synthetic source mimicking the field source is propagated computationally through a smooth medium, and the recorded wavefield is backpropagated through this same medium. The image is often taken to be the zero time lag crosscorrelation between the two fields.

Along with other common seismic processing and migration methods, RTM relies on the single-scattering assumption. Data with multiples create spurious structures in the final image since they cannot be propagated back to the correct scattering location without already knowing the scattering locations. Multiples must therefore be removed prior to migration. Several methods exist to suppress free-surface-related and internal multiples from prestack data, as described for example in Ikelle and Amundsen (2005).

Other methods account for multiples during the migration process, and may even use them to enhance the final image (Schuster et al., 2004; Berkhout and Verschuur, 2006; Malcolm et al., 2009; Berkhout, 2012). One particular method, the Marchenko method (Wapenaar et al., 2013, 2014) has been developed to remove the effect of multiples in the image. It works by solving a so-called Marchenko equation that relates surface reflection data and transmission estimates (e. g. direct waves from the surface to an imaging location in the subsurface), to the main sought-after wavefields which are the surface-to-subsurface Green's functions and focusing functions. A focusing function is a solution of the wave equation which propagates through a reference medium in such a way that it reaches a specified focusing depth as a delta function in time and space. The reference medium in which it is defined is reflection-free below the focusing depth so the focus then diverges as a downgoing field through the reflection-free part of the reference medium.

Marchenko methods have recently been used for a variety of purposes, including imaging (Wapenaar et al., 2014; da Costa Filho et al., 2015; Singh et al., 2015), internal multiple attenuation (Meles et al., 2015; da Costa Filho et al., 2017), redatuming and target-oriented imaging (Wapenaar et al., 2014; Ravasi et al., 2016), and virtual subsurface wavefield estimation (Wapenaar et al., 2016). One particular application which has been developed by Meles et al. (2016) synthesizes prestack primaries from the subsurface Green's functions obtained by the Marchenko method. It therefore generates data suitable for any method relying on a single-scattering assumption, such as RTM.

Using focusing functions as opposed to Green's functions to obtain artifact-free images has also been investigated (Meles et al., 2017; da Costa Filho et al., 2017). They consider virtual acquisitions defined by the focusing functions, and then use their special properties to extract information about individual reflectors. Here, we show novel results in acoustic and elastic media. In addition, we combine the images using the method of da Costa Filho and Curtis (2016) to provide images with almost no acquisition or multiple-related artifacts.

Theory

The Marchenko method provides Green's functions as well as focusing functions denoted $f_1(\mathbf{x}_0, \mathbf{x}_F, t)$ where $\mathbf{x}_0$ is at the surface, $\mathbf{x}_F$ is the focusing location and t is time (Wapenaar et al., 2014). These are defined in a reference medium which is reflection-free below $\mathbf{x}_F$, and equal to the true medium between the surface and the focusing depth. They have the characteristic that, at zero-time, the wavefield at the depth of $\mathbf{x}_F$ focuses, that is, it becomes a band-limited delta function at $\mathbf{x}_F$. These functions are commonly decomposed with regard to their directions of propagation

related to their first argument. Therefore, $f_1^+(\mathbf{x}_0,\mathbf{x}_F,t)$ refers to the downgoing field departing from $\mathbf{x}_0$, and $f_1^-(\mathbf{x}_0,\mathbf{x}_F,t)$ is the upgoing field arriving at $\mathbf{x}_0$ when one creates a focus at $\mathbf{x}_F$. Green's function G is similarly decomposed into G^- and G^+.

Focusing functions are related to the surface reflection data $R(\mathbf{x}_0'',\mathbf{x}_0,t)$, and the subsurface Green's function, $G^-(\mathbf{x}_F,\mathbf{x}_0'',t)$, by the equation (Wapenaar et al., 2014)

$$G^-(\mathbf{x}_F,\mathbf{x}_0'',t) = -f_1^-(\mathbf{x}_0'',\mathbf{x}_F,t) + \int_{\partial\mathbb{D}_0}\int_{-\infty}^{\infty} R(\mathbf{x}_0'',\mathbf{x}_0,t-\tau) f_1^+(\mathbf{x}_0,\mathbf{x}_F,\tau)\,\mathrm{d}\tau\,\mathrm{d}^2\mathbf{x}_0. \quad (1)$$

In the equation above, some quantities are defined in the real medium, while others are defined in the reference medium. If we consider them all in the reference medium then $G^-(\mathbf{x}_F,\mathbf{x}_0'',t)=0$ at the focusing depth, and thus

$$f_1^-(\mathbf{x}_0',\mathbf{x}_F',t) = \int_{\partial\mathbb{D}_0}\int_{-\infty}^{\infty} \overline{R}(\mathbf{x}_0',\mathbf{x}_0,t-\tau) f_1^+(\mathbf{x}_0,\mathbf{x}_F',\tau)\,\mathrm{d}\tau\,\mathrm{d}^2\mathbf{x}_0 \quad (2)$$

where $\overline{R}(\mathbf{x}_0',\mathbf{x}_0,t)$ is the reflection response in the reference medium.

A direct consequence of this is that an f_1^+ source (for a fixed $\mathbf{x}_F$) produces an f_1^- field measured along $\partial\mathbb{D}_0$. Simply put, f_1^- is the reference medium response to f_1^+.

The Marchenko method is thus also useful for producing focusing functions, which are essentially virtual data acquisitions that take place in an imagined medium, which contains the true medium above the focusing depth. Here, we explore some of interesting properties of these virtual acquisitions derived from the focusing functions. We propose imaging methods which exploit these acquisitions, including one to image specific reflectors.

Methods

In RTM a forward source is propagated in a medium that is a best-possible approximation to the true medium, and the received wavefield is backpropagated through the same medium. The two wavefields are combined to construct an image. With a virtual acquisition, the same process can be employed. However, we may use $f_1^+(\mathbf{x}_0,\mathbf{x}_F,t)$ as a source field injected along the whole surface source array, as opposed to a point source at a specific location. In this case, the "measured" data is $f_1^-(\mathbf{x}_0,\mathbf{x}_F,t)$.

The nature of the focusing source/receiver pair will have two effects on the image produced using a single virtual focus point $\mathbf{x}_F$. First, it will be localized as the source does not expand outwardly, but focuses towards the focus point. Second, since it is defined in the reference medium, it will not image anything below $\mathbf{x}_F$. In light of this, in order to image the medium using these virtual surveys, one has to compute the image for several focus points in order to illuminate the whole subsurface, and these must be placed below the deepest target reflector.

Slob et al. (2014) and Wapenaar et al. (2014) show how $f_1^+(\mathbf{x},\mathbf{x}_F,t)$ contains a time-reversed direct wave $f_{1,d}^+$, which scatters as it propagates through the reference medium, and a coda $f_{1,m}^+$ which destructively interferes with this scattering. $f_{1,m}^+$ does this in such way that the only arrival reaching the focusing depth is the time-reversed direct wave; this arrives at $\mathbf{x}_F$ and $t=0$. Moreover, Meles et al. (2017) have shown that a direct consequence of focusing is that *only primaries* are present in f_1^-. Indeed, any multiple not destroyed by $f_{1,m}^-$ would propagate downwards to destroy the focus. Since f_1^- is composed of only primaries, and $f_{1,d}^+$ creates both primaries and multiples, it follows that some of the primaries in f_1^- are created by $f_{1,d}^+$, and the rest are created by $f_{1,m}^+$.

However, since the direct wave $f_{1,d}^+$ illuminates all reflectors in the reference medium, to image it we need only propagate $f_{1,d}^+$, as opposed to propagating the full f_1^+. This reduces crosstalk between unrelated events in $f_{1,m}^+$ and f_1^-. Unfortunately, since f_1^- still contains primaries from $f_{1,m}^+$, not all artifacts are eliminated. However, these artifacts will be, in general, at different locations than multiple-related artifacts in RTM. Thus, we can exploit these differences to attenuate artifacts by using the combined-images method of da Costa Filho and Curtis (2016)

It can be shown (Meles et al., 2017) that in 1D media, the last arriving event in f_1^- is a primary created by $f_{1,d}^+$. Therefore, for any given focus point $\mathbf{x}_F$, we may generate an upgoing focusing gather $f_1^-(\mathbf{x}_0,\mathbf{x}_F,t)$ such that the last event of this gather will be a primary, $f_{1,p}^-(\mathbf{x}_0,\mathbf{x}_F,t)$, originating from a known source, $f_{1,d}^+(\mathbf{x}_0,\mathbf{x}_F,t)$. This allows us to migrate only primaries by considering source/receiver pairs composed of $f_{1,d}^+$ and $f_{1,p}^-$. The primary recovered will image the closest reflector immediately above the focusing location; if all reflectors are to be imaged, subsurface focus points must be located below every reflector.

The methods shown for acoustic media have a straightforward extension to elastic media, with certain caveats which we highlight below with the synthetic 1.5D model in Figure 3a. da Costa Filho et al. (2014), Wapenaar (2014) and Wapenaar and Slob (2014) have shown how focusing functions may be computed in elastic media. Consequently, these methods which do not require windowing may be used to compute elastic images by migrating source/receiver pairs composed of down- and upgoing elastic focusing functions.

The method above which requires windowing f_1^- to obtain $f_{1,p}^-$ fields cannot be extended as easily to elastic media. In particular, the assumption that the last arriving wave is a pure-mode primary used for acoustic media does not hold for all wave types. A focus originating from a compressional time-reversed direct wave will create not only P waves, but also conversions which will arrive at or after the last pure-mode P primary in the upgoing focusing functions: these have certainly reflected only once, but they also forward-scatter through conversion, making them noncompliant with the first-order Born assumption and harder to migrate. However, the assumption is valid for S-wave foci: the last event arriving in the upgoing field created by an S direct wave will also be a pure-mode S wave. Any conversion into P will have traveled faster than the pure S wave. As such, the third method of primaries can be extended directly to pure-mode S waves in elastic media.

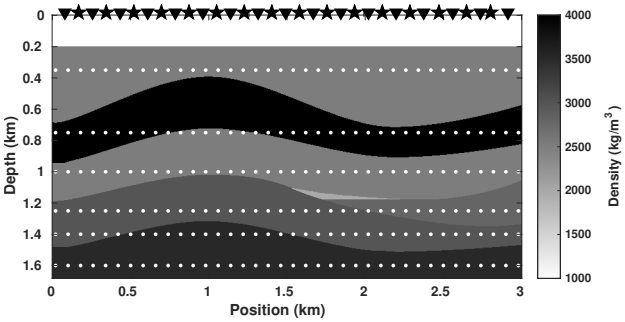

Figure 1: Acquisition and imaging geometry for 2D synthetic model. Stars and triangles represent colocated surface sources and receivers. White dots represent locations where $f_1^{\pm}$ were computed.

Results

Acoustic

We test the methods using a 2D synthetic acoustic model with a constant velocity of $2400\,\mathrm{m/s}$ and densities shown in Figure 1. We compute focusing functions at several depth levels as shown in Figure 1. The bottommost depth level at $1150\,\mathrm{m}$ is used for imaging with the pair $f_{1,d}^{+}$ and f_1^{-}, displayed in Figure 2a; in this case, the Marchenko reference medium has the same reflectors as the full medium. The other depth levels are used to image with primaries in Figure 2d, that is, using $f_{1,d}^{+}$ and $f_{1,p}^{-}$. In order to recover all reflectors using only primaries, focus points below each interface are necessary.

As expected, Figures 2a contains a few artifacts resulting from crosstalk. However, standard RTM shown in Figure 2b contains significantly stronger and more numerous artifacts compared to Figure 2a. Since these artifacts appear in different locations, we combined the focusing image with the standard RTM image to generate the combined-image in Figure 2c. This image is virtually free from artifacts, and has fewer acquisition imprints than its constituent images.

Figure 2d also shows near perfect reconstruction of primaries. No coherent spurious interfaces are imaged, and all true reflectors have been recovered. However, this performance comes at the cost of picking the last event in f_1^{-} (in this case performed automatically), as well as an increased computational cost.

Elastic

We use a 1.5D synthetic elastic model with a constant P velocity of $2500\,\mathrm{m/s}$, constant S velocity of $1300\,\mathrm{m/s}$, and densities shown in Figure 3. We compute focusing functions at the depth level shown in Figure 3.

Next, we compute the SS images corresponding to imaging pair $f_{1,d}^{+}$ and f_1^{-} (Figure 4a) and standard RTM (Figure 4b). These images are combined to generate the image in Figure 4c. In Figure 4d we see the image generated by imaging pair $f_{1,d}^{+}$ and $f_{1,p}^{-}$ for the single boundary of focus locations in our model.

Our first method (Figure 4a), as in the acoustic case, is comparable to RTM (Figure 4a) in terms of artifacts. While it contains fewer acquisition imprints, it still contains a few

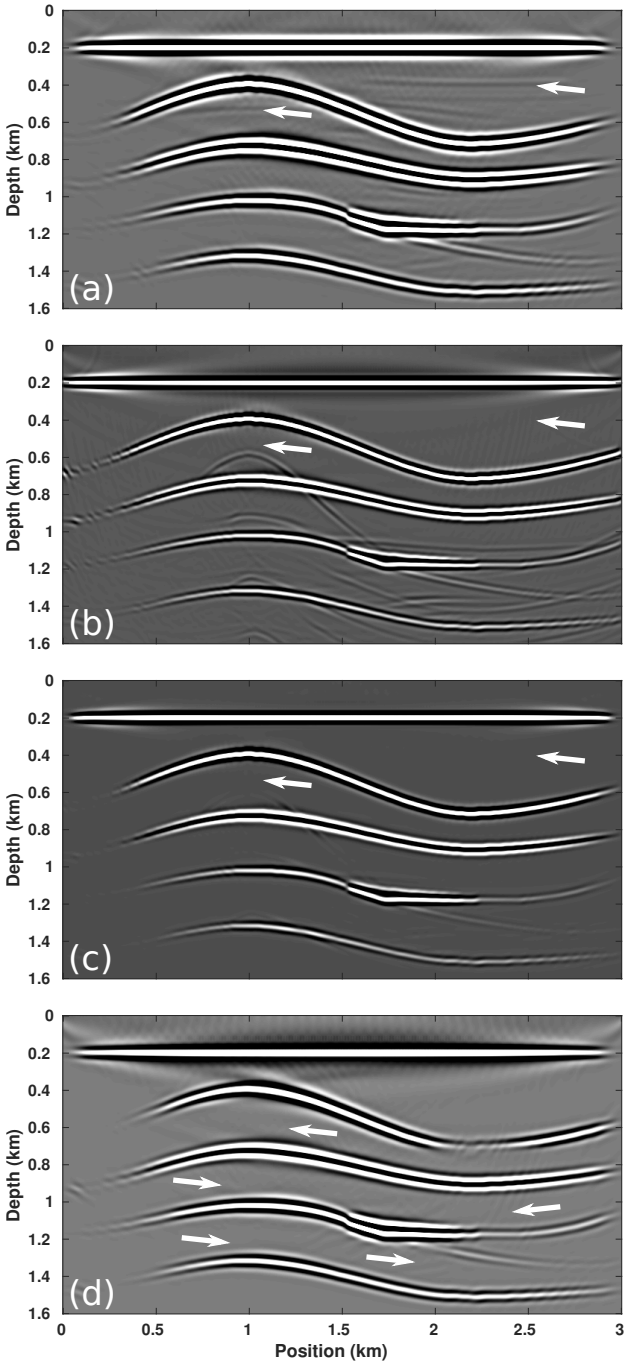

Figure 2: Images constructed using source/receiver wavefields (a) $f_{1,d}^{+}$ and f_1^{-}, and (d) $f_{1,d}^{+}$ and $f_{1,p}^{-}$. (b) Conventional RTM image. (c) Combined image from images in panels (a) and (b). Image in (a) uses only focus points in the bottommost line in Figure 1 and (d) uses all focus points. Arrows indicate spurious reflectors.

spurious reflectors. Combining these two images, however, shows near-perfect recovery of the true interfaces. In addition, imaging only the last primary in f_1^{-} also provides an artifact-free image of an individual reflector.

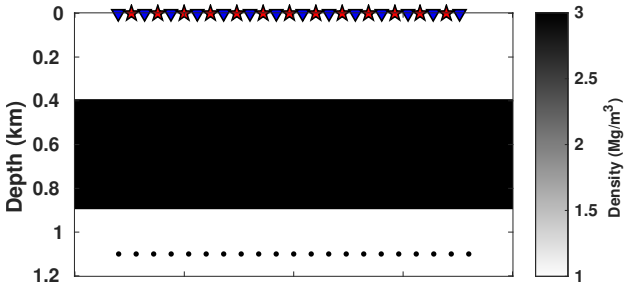

Figure 3: 1.5D density model used for elastic data. Colocated sources and receivers are shown as stars and triangles, and the focus point locations are shown as dots.

Discussion

These results demonstrate the advantages and limitations of the new imaging methods. The first method uses $f_{1,d}^{+}$ and f_{1}^{-} along a boundary of focusing locations as source/receiver wavefield pairs to create the image. It provides images that are inherently different from those obtained from standard RTM, provided that focusing is achieved with low levels of error in the Marchenko method.

In both the acoustic and elastic synthetic models, artifacts mostly appear in different locations from RTM, suggesting that the focusing achieved was acceptable. Our first method exhibits some crosstalk between $f_{1,d}^{+}$ and unrelated events in f_{1}^{-}. Nevertheless, these artifacts are weaker and fewer than in RTM for acoustic media, and for elastic media, comparable to those in RTM. To reduce them, we combined the RTM image with our Marchenko focusing image using the combined imaging method of da Costa Filho and Curtis (2016). This provides images with near-perfect recovery of interfaces in both tested models, lacking multiple-related artifacts and acquisition artifacts alike.

Our final imaging method uses the windowed f_{1}^{-} functions, denoted $f_{1,p}^{-}$; these retain only their last events which are primaries related to the reflector immediately above the focus point. This method allows the imaging of individual reflectors without interference from other parts of the wavefield. However, if an image of the entire medium is desired, each reflector must be imaged separately which in turn requires more computational power to calculate focusing functions at more focus points. Nevertheless, it has been shown to provide clean images of individual reflectors. The picking as done automatically, but for field data may have to be done manually. This was the approach of da Costa Filho et al. (2017), so as to ensure consistent arrivals across focusing gathers. This increases processing time significantly, and hence this method may be most applicable for target-oriented applications, this extra time may be worthwhile if it better images a reservoir.

These three methods provide significant insights into several areas of active research in seismics. In standard RTM, one assumes that the point-source function only creates primaries. This is known as the linearization, or first-order Born approximation, whereby the receiver wavefield created by the source function is linearly related to the medium parameters.

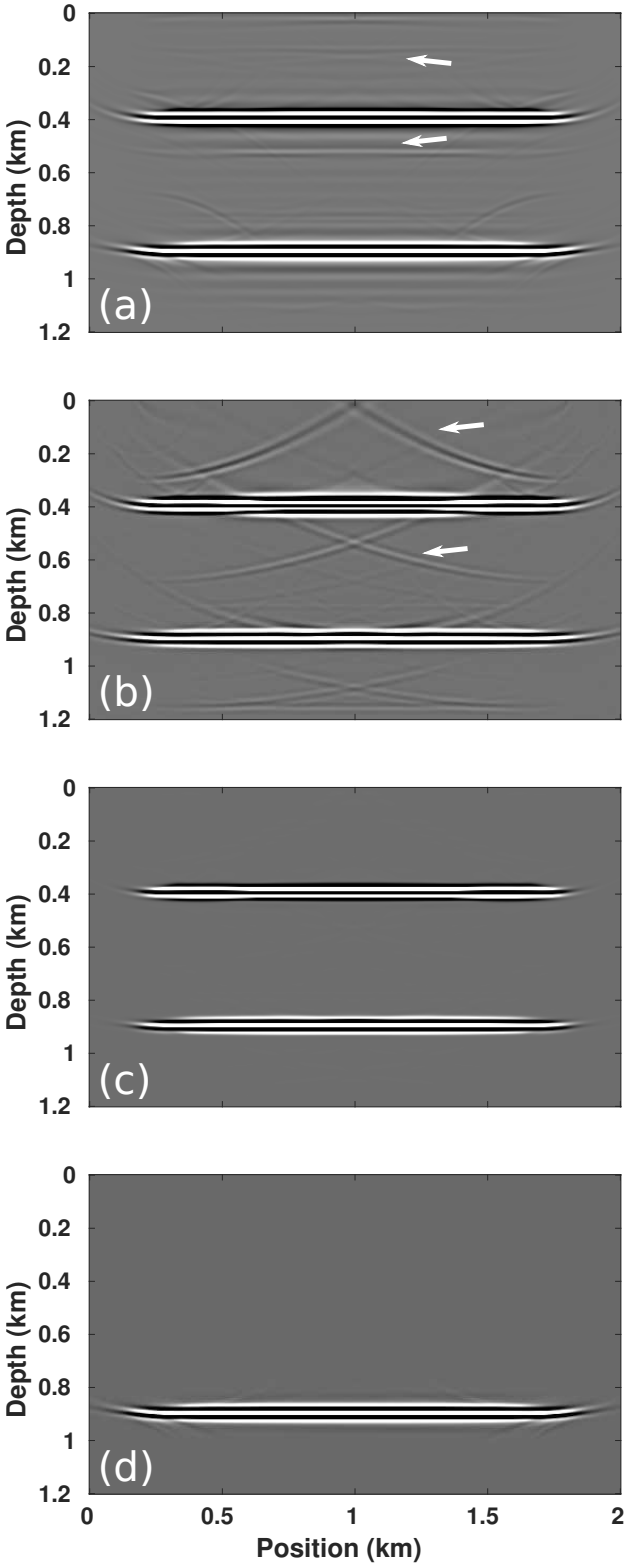

Figure 4: SS images using source/receiver wavefields (a) $f_{1,d}^{+}$ and f_{1}^{-}, and (d) $f_{1,d}^{+}$ and $f_{1,p}^{-}$. RTM is shown in (b) and the combined image between (a) and (b) is shown in (c).

In order for this approach to be valid, data used in standard RTM must be demultipled. The source function f_{1}^{+} creates all events in f_{1}^{-}. Indeed, since all events in f_{1}^{-} are

primaries, this imaging method is truly linear in the sense that events in f_1^- are linearly related to the source function (f_1^+) by the reference medium parameters. This is achieved without any multiple removal. However, obtaining $f_1^{+/-}$ is a nonlinear process.

Using $f_{1,d}^+$ instead of f_1^+, while not fully respecting wave propagation ($f_{1,d}^+$ does not generate f_1^-), has been shown to be a useful approximation in terms of imaging. Indeed, combining this imaging condition with RTM generates almost perfect images.

The last method is also excellent at obtaining clean images, and can be seen as imaging a subset of a truly linear method which would use $f_{1,d}^+$ as source and only its related primaries in f_1^- as the received wavefield.

The behavior of focusing functions allows structures to be targeted with a small number of focus points, reducing imaging cost of certain areas. In addition, we generate images with fewer artifacts without multiple removal, and at much lower computational expense than Marchenko redatuming and imaging. At the cost of performing both conventional and focusing RTM, combined images are exceptionally clean. As such, these methods can be target oriented to investigate, for example, known reservoirs. Moreover, the first method can be used to substitute for demultiple plus RTM, Marchenko redatuming plus RTM, and Marchenko imaging, especially for geologies which generate many multiples. Our methods are computationally cheap compared to Marchenko imaging and more efficient than standard RTM.

Conclusions

We have presented novel methods to image subsurface structures using specially crafted virtual acquisitions. These acquisitions are given by the outputs of the Marchenko method, and are composed of source/receiver wavefields given by the down- and upgoing focusing functions, respectively. Additionally, we present a method based on these acquisitions which can image individual reflectors: this method involves windowing upgoing focusing functions based on generally-applicable properties of the traveltimes of events in focusing functions. We apply these methods to acoustic 2D synthetic data, and to elastic 1.5D synthetic data. We discuss the advantages and limitations of the methods, as well as implications they might have to other areas of seismic processing.

Acknowledgments

The authors thank the Edinburgh Interferometry Project sponsors (Schlumberger Gould Research, Statoil and Total) for supporting this research. The first author also thanks CAPES for funding.

References

Berkhout, A. J., 2012, Combining full wavefield migration and full waveform inversion, a glance into the future of seismic imaging: Geophysics, **77**, S43–S50.

Berkhout, A. J., and D. J. Verschuur, 2006, Imaging of multiple reflections: Geophysics, **71**, SI209–SI220.

da Costa Filho, C. A., and A. Curtis, 2016, Attenuating multiple-related imaging artifacts using combined imaging conditions: Geophysics, **81**, S469–S475.

da Costa Filho, C. A., G. A. Meles, and A. Curtis, 2017, Elastic internal multiple analysis and attenuation using Marchenko and interferometric methods: Geophysics, **82**, Q1–Q12.

da Costa Filho, C. A., G. A. Meles, A. Curtis, M. Ravasi, and A. Kritski, 2017, Imaging strategies using 2D acoustic and elastic Marchenko focusing functions: 79th EAGE Conference & Exhibition, submitted.

da Costa Filho, C. A., M. Ravasi, and A. Curtis, 2015, Elastic P- and S-wave autofocus imaging with primaries and internal multiples: Geophysics, **80**, S187–S202.

da Costa Filho, C. A., M. Ravasi, A. Curtis, and G. A. Meles, 2014, Elastodynamic Green's function retrieval through single-sided Marchenko inverse scattering: Physical Review E, **90**, 063201.

Ikelle, L. T., and L. Amundsen, 2005, Introduction to petroleum seismology. Investigations in Geophysics.

Malcolm, A. E., B. Ursin, and M. V. de Hoop, 2009, Seismic imaging and illumination with internal multiples: Geophysical Journal International, **176**, 847–864.

Meles, G. A., C. A. da Costa Filho, and A. Curtis, 2017, Estimating and imaging with primaries constructed from single-sided focusing wavefields: 79th EAGE Conference & Exhibition, submitted.

Meles, G. A., K. Löer, M. Ravasi, A. Curtis, and C. A. da Costa Filho, 2015, Internal multiple prediction and removal using Marchenko autofocusing and seismic interferometry: Geophysics, **80**, A7–A11.

Meles, G. A., K. Wapenaar, and A. Curtis, 2016, Reconstructing the primary reflections in seismic data by Marchenko redatuming and convolutional interferometry: Geophysics, **81**, Q15–Q26.

Ravasi, M., I. Vasconcelos, A. Kritski, A. Curtis, C. A. da Costa Filho, and G. A. Meles, 2016, Target-oriented Marchenko imaging of a North Sea field: Geophysical Journal International, **205**, 99–104.

Schuster, G. T., J. Yu, J. Sheng, and J. Rickett, 2004, Interferometric/daylight seismic imaging: Geophysical Journal International, **157**, 838–852.

Singh, S., R. Snieder, J. Behura, and J. van der Neut, 2015, Marchenko imaging: Imaging with primaries, internal multiples, and free-surface multiples: Geophysics, **80**, S164–S174.

Slob, E., K. Wapenaar, F. Broggini, and R. Snieder, 2014, Seismic reflector imaging using internal multiples with Marchenko-type equations: Geophysics, **79**, S63–S76.

Wapenaar, K., 2014, Single-sided Marchenko focusing of compressional and shear waves: Physical Review E, **90**, 063202.

Wapenaar, K., F. Broggini, E. Slob, and R. Snieder, 2013, Three-Dimensional Single-Sided Marchenko Inverse Scattering, Data-Driven Focusing, Green's Function Retrieval, and their Mutual Relations: Physical Review Letters, **110**, 084301.

Wapenaar, K., and E. Slob, 2014, On the Marchenko equation for multicomponent single-sided reflection data: Geophysical Journal International, **199**, 1367–1371.

Wapenaar, K., J. Thorbecke, J. van der Neut, F. Broggini, E. Slob, and R. Snieder, 2014, Marchenko imaging: Geophysics, **79**, WA39–WA57.

Wapenaar, K., J. van der Neut, and E. Slob, 2016, Unified double- and single-sided homogeneous Green's function representations: Proceedings of the Royal Society A: Mathematical, Physical and Engineering Science, **472**, 20160162.